Tellus (2006)

TELLUS

Climate-carbon cycle feedbacks under stabilization: uncertainty and observational constraints

By CHRIS D. JONES[1*], PETER M. COX[2] and CHRIS HUNTINGFORD[3], [1]*Hadley Centre, Met Office, Exeter EX1 3PB, UK;* [2]*Centre for Ecology and Hydrology, Winfrith, Dorset DT2 8ZD, UK;* [3]*Centre for Ecology and Hydrology, Wallingford, Oxon OX10 8BB, UK*

(Manuscript received 12 January 2006; in final form 29 June 2006)

ABSTRACT

Avoiding 'dangerous climate change' by stabilization of atmospheric CO_2 concentrations at a desired level requires reducing the rate of anthropogenic carbon emissions so that they are balanced by uptake of carbon by the natural terrestrial and oceanic carbon cycles. Previous calculations of profiles of emissions which lead to stabilized CO_2 levels have assumed no impact of climate change on this natural carbon uptake. However, future climate change effects on the land carbon cycle are predicted to reduce its ability to act as a sink for anthropogenic carbon emissions and so quantification of this feedback is required to determine future permissible emissions. Here, we assess the impact of the climate-carbon cycle feedback and attempt to quantify its uncertainty due to both within-model parameter uncertainty and between-model structural uncertainty. We assess the use of observational constraints to reduce uncertainty in the future permissible emissions for climate stabilization and find that all realistic carbon cycle feedbacks consistent with the observational record give permissible emissions significantly less than previously assumed. However, the observational record proves to be insufficient to tightly constrain carbon cycle processes or future feedback strength with implications for climate-carbon cycle model evaluation.

1. Introduction

As atmospheric concentrations of greenhouse gases, and in particular CO_2, increase this will cause major changes in climate (IPCC-TAR; Houghton et al., 2001). For some regions of the world, this may ultimately lead, to 'dangerous climate change' (Pachauri, 2006; Schneider and Lane, 2006) and so stabilization scenarios are receiving increasing amounts of interest both politically and scientifically (Knutti et al., 2005; Matthews, 2005; Jones et al., 2006).

The degree to which a given level of global climate change can be considered dangerous is impossible to define precisely, with both gradual and sudden impacts becoming more likely and more severe for greater levels of change (McCarthy et al., 2001). Similarly, translating a level of climate change into a level of CO_2 is difficult. Large uncertainty remains in climate sensitivity, and so a probabilistic approach to determining a safe level of CO_2 is required (Mastrandrea and Schneider, 2006; Meinshausen, 2006). Here, we do not attempt to quantify what level of atmospheric CO_2 constitutes dangerous change, but choose to assess two commonly considered levels of stabilization—namely 450 and 550 ppm—in terms of the impact of climate-carbon cycle feedbacks on the permissible emissions required to achieve stabilization.

We use a coupled climate-carbon cycle model to calculate anthropogenic CO_2 emission profiles that would lead to a stable atmospheric CO_2 concentration. The emissions profiles derived will be highly dependent on the sensitivity of the natural carbon cycle to both climate change and to atmospheric CO_2 itself.

Previous studies with coupled climate carbon cycle models (Cox et al., 2000; Friedlingstein et al., 2001; Thompson et al., 2004; Zeng et al., 2004) have suggested that the terrestrial biosphere will become a less effective net sink of carbon, and may even become a source. Soil respiration rates increase for higher temperatures and eventually exceed the increased vegetation productivity at higher atmospheric CO_2 concentrations. This positive climate-carbon cycle feedback significantly reduces the ability of the natural terrestrial ecosystem to offset anthropogenic CO_2 emissions.

There is an increasing consensus that climate-carbon cycle feedbacks will decrease the uptake capacity of the natural carbon cycle. Friedlingstein et al. (2006) present results from C4MIP, the Coupled Climate Carbon Cycle Model Intercomparison Project, and show that all 11 models exhibit positive climate-carbon cycle feedbacks. Such studies on the impact of climate on the carbon

*Corresponding author.
e-mail: chris.d.jones@metoffice.gov.uk
DOI: 10.1111/j.1600-0889.2006.00215.x

cycle generally focus on the impact of the feedbacks on elevated atmospheric CO_2 levels for a given scenario of carbon emissions. However, the same scientific principal leads to the converse result that for a given profile of atmospheric CO_2 level, the impacts of climate change will reduce the level of anthropogenic emission required to achieve it. Chapter 3 of the IPCC's Third Assessment Report (TAR) (Prentice et al., 2001) briefly alludes to the impact of climate-carbon cycle feedbacks on stabilization emissions but does not quantify the associated magnitude of emissions reductions. Joos et al. (1999) used a simplified model to quantify the ocean carbon cycle impact but did not discuss the terrestrial behaviour. Friedlingstein et al. (2001) show how positive feedbacks in a coupled carbon cycle general circulation model (GCM) reduce the emissions required to stabilize atmospheric CO_2 in an idealized $4 \times CO_2$ experiment.

Recently, this issue has been re-addressed using two coupled climate-carbon cycle models (Matthews, 2005, 2006; Jones et al., 2006) which both predict substantial reductions in permissible emissions. Here, we extend the work of Jones et al. (2006) to consider the implications of the large uncertainties in the feedbacks due to both uncertainty in the sensitivity of the terrestrial carbon cycle to climate (Friedlingstein et al., 2006) and of the climate sensitivity to atmospheric CO_2 (Andreae et al., 2005) and assess whether the observational record can constrain the behaviour and reduce uncertainty in future permissible emissions.

The results show that the permissible emissions to achieve CO_2 stabilization may be much lower than previously calculated as a result of climate-carbon cycle feedbacks. The non-uniqueness of stabilization pathways is not considered in this study, but there are clearly many CO_2 profiles, and associated emissions, to stabilize at a given level. For example Matthews (2006) investigate both SP550 and DSP550 scenarios (Knutti et al., 2005) which propose different pathways to stabilization at 550 ppmv. Our initial analysis, however, indicates that the cumulative emissions to stabilize by different pathways may be relatively insensitive to the chosen pathway.

The simple model we use is outlined in Section 2 and described in detail in the Appendix. Section 3 describes the experimental design and presents results of single parameter perturbations. Section 4 presents results from multiple parameter perturbations and discusses to what extent the observational record can constrain the model behaviour, and Section 5 presents uncertainty from intermodel comparison. Conclusions are given in Section 6.

2. Modelling and incorporation of uncertainty

HadCM3LC is a configuration of the Hadley Centre GCM (HadCM3, Gordon et al., 2000), extended to include a fully interactive representation of the global carbon cycle (Cox et al., 2000, 2001). It has been used to investigate the consequences of climate-carbon cycle feedbacks for permissible emissions required to achieve stabilization (Jones et al., 2006), finding that the emissions required to achieve the prescribed WRE450 and WRE550 CO_2 profiles (Wigley et al., 1996) show a marked reduction when carbon cycle feedbacks are included.

Here, we explore the uncertainties in the above result using a simple climate-carbon cycle model (Jones et al., 2003b), calibrated and tested against HadCM3LC simulations as described by Jones et al. (2006). For full details, see the Appendix. To better represent the temporal response of climate to CO_2, we incorporate a simple heat capacity term into the model as done by Andreae et al. (2005).

By calibrating the simple model against the response from the GCM in terms of global mean temperature, we are implicitly including both the global and regional effects of temperature and precipitation. Such a pattern scaling approach was adopted and described in more detail in Huntingford and Cox (2000). Hence the parametrizations presented here should not be considered so much as representing a direct response to temperature in a physiological sense, but rather a large-scale response of the ecosystem to climate change in general. In other words, the simple model implicitly includes the effects of climate variables other than temperature, such as hydrological changes which are clearly very important in determining ecosystem functioning and carbon balance. However, the relation of such variables to temperature is dependent on the GCM used for the calibration of the simple model. It is beyond the scope of this study to explore the different hydrological sensitivities to temperature, but such uncertainty may be important in determining regional and global carbon budgets.

The simple model's capability to perform many simulations allows examination of the key uncertain parameters within the terrestrial carbon cycle system which determine the size of the climate-carbon cycle feedback. Here, we use the simple model to perform multiple experiments using prescribed atmospheric CO_2 levels. The model diagnoses the anthropogenic emissions required to attain the CO_2 profile taking into account the impact of climate change and CO_2 level on carbon cycle behaviour. Historical CO_2 levels were prescribed from 1860 to 2000 and subsequent CO_2 levels from WRE450 and WRE550 stabilization scenarios up to 2300. During the historical period global mean temperature was prescribed according to Parker et al. (1995). After 2000, temperature is computed in the model using the heat capacity equation of Andreae et al. (2005) with a heat capacity of $1.1\ \mathrm{GJ\,m^{-2}\,K^{-1}}$. Climate forcing due to sulphate aerosol and non-CO_2 greenhouse gases is implicit during the historical period due to the prescribed global mean temperature. At year 2000 the strength of aerosol forcing is diagnosed to be consistent with the prescribed climate change and the chosen climate sensitivity for each experiment. Aerosol forcing is then assumed to fall smoothly to zero by 2100 and remain at zero thereafter. No other climate forcings are altered after present day.

The model is described in detail in the Appendix, but the main parameters under consideration in this study are described here:

(1) Productivity sensitivity to CO_2. Ecosystem response to increasing atmospheric CO_2, C_a, is represented using a half-saturation constant, $C_{0.5}$, defined as the CO_2 level at which gross primary productivity (GPP), Π, reaches half its maximum value:

$$\Pi = \Pi_{\max} \left(\frac{C_a}{C_a + C_{0.5}} \right) f(T) \tag{1}$$

Higher values of $C_{0.5}$ imply greater CO_2 fertilization as the increase in Π for a given C_a increases with $C_{0.5}$.

(2) Respiration sensitivity to climate. A simple exponential 'Q10' sensitivity of heterotrophic respiration to temperature, where the parameter, q_{10}, gives the fractional increase in respiration for a 10° warming (see e.g. Knorr et al., 2005):

$$R_s(T) = \kappa C_s q_{10} \left(\frac{T - T_0}{10} \right)^{K} \tag{2}$$

given soil carbon, C_s and a rate constant, κ.

(3) Productivity sensitivity to climate. The response of vegetation growth to climate change in terms of global mean temperature change relative to pre-industrial, $(T - T_0)$, is parametrized here as a quadratic function

$$f(T) = 1 + b(T - T_0) + c(T - T_0)^2, \tag{3}$$

where $f(T)$ is used in eq. (1) to calculate producitivty. Instead of considering values of b and c which have little intuitive meaning, we characterize this parametrization by curvature, d^2GPP/dT^2, and optimum temperature, T_{opt}, relative to T_0.

Fitting the simple model to the HadCM3LC simulation of Cox et al. (2000), we obtain parameter values of $q_{10} = 2.0$, $C_{0.5} = 466$ ppm, $d^2GPP/dT^2 = -0.011\ K^{-2}$ and $T_{opt} = 0K$. HadCM3LC has a climate sensitivity of about 3.0K for a doubling of atmospheric CO_2. Jones et al. (2006) show how well the simple model calibrated against a transient GCM simulation recreates the GCM's stabilization simulations.

3. Quantifying uncertainty in climate-carbon cycle feedbacks

To assess the impact of parameter uncertainty, model simulations are performed varying each of the four terrestrial response parameters singly within the following ranges: $C_{0.5}$ from 250 to 1000 ppm, q_{10} from 1 to 4, d^2GPP/dT^2 from 0 to $-0.024\ K^{-2}$ and T_{opt} from -3 to 3 K. While each parameter is perturbed, the other parameters are held constant at the values derived from calibration against HadCM3LC.

The parameter ranges we choose to consider are somewhat arbitrary, and are intentionally large (e.g. it is very unlikely that on a global mean scale, q_{10} is as low as 1 or as large as 4 (Jones and Cox, 2001)). It is not our intention to restrict, a priori, the range considered but rather to span the whole range of plausible behaviour from very high sensitivity to CO_2 and climate to very low sensitivity. In this way, we hope to reduce the problem of our results being too model specific, although missing processes in a model cannot be compensated for by large parameter ranges. Section 4 will assess whether comparison with the observational record allows us to constrain model behaviour and narrow the parameter range considered.

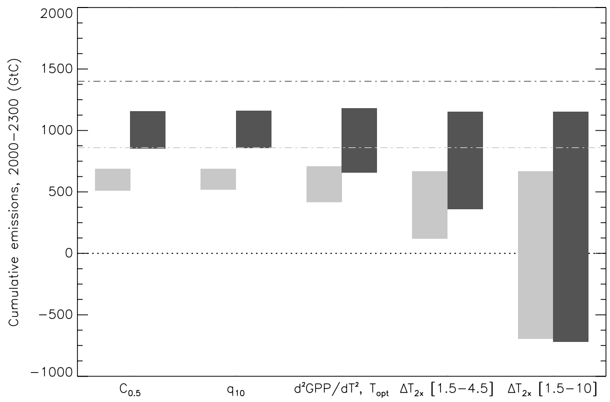

Fig. 1. Uncertainty in cumulative permissible emissions from 2000 to 2300 due to uncertainty in the carbon cycle sensitivity to CO_2 or climate, and climate sensitivity. The bars show the range of cumulative emissions when each parameter is varied individually within the range stated in the text. Results are shown for climate sensitivity values from 1.5 to 4.5 K, and from 1.5 to 10 K. Pale bars show results for stabilization at 450 ppm following the WRE450 CO_2 scenario, and dark bars likewise for WRE550. The dashed lines represent the level of cumulative emissions from Wigley et al. (1996).

Figure 1 shows how varying each parameter alone affects total permissible emissions to stabilize at 450 and 550 ppm. For each parameter, and each stabilization level, the bars show the uncertainty range of cumulative emissions resulting from varying that parameter alone within its prescribed range. For each process, there is a large spread of uncertainty in permissible emissions, with sensitivity of productivity to climate, GPP(T), being the most important carbon cycle response when varied within our chosen ranges. This is in agreement with the conclusions of Matthews et al. (2005), but is clearly also dependent on our arbitrary choice of the extent of the parameter ranges.

Significant uncertainty also exists in climate sensitivity—the change in global mean temperature expected for a doubling of atmospheric CO_2. A high climate sensitivity implies greater climate change for a given stabilization level of CO_2. Neither modelling studies (based on multiple GCM simulations with multiple perturbations of parameters; Murphy et al., 2004; Stainforth et al., 2005) nor observationally based studies (Andronova and Schlesinger, 2001; Forest et al., 2002; Gregory et al., 2002; Harvey and Kaufmann, 2002; Knutti et al., 2002) have been able to constrain the climate sensitivity. In particular, due to large uncertainty in the cooling strength of aerosols, neither approach is able to rule out the possibility of climate sensitivity significantly greater than the range of 1.5–4.5 K reported by the IPCC-TAR, with the 95% confidence limits of some of the probability density functions exceeding 10 K. This implies a small, but non-zero possibility of very large longterm warming. More recently, constraints from considering temperature during the last millenium (Hegerl et al., 2006) and changes since the Last Glacial Maximum (Annan et al., 2005; von Deimling et al., 2006) imply a lowered upper limit of climate sensitivity closer to 6 K. Combining such independent evidence makes high climate sensitivity even less likely (Annan and Hargreaves, 2006), but the large potential impacts of high sensitivity mean such possibilities should not be discounted. Hence, our investigation examines a range of likely climate sensitivity from 1.5 to 4.5 K and also a more extreme range from 1.5 to 10 K.

To explore the impact of this uncertainty in the simple model we first vary climate sensitivity, $\Delta T_{2\times}$, within the IPCC-TAR range of 1.5–4.5 K. We find a spread of permissible emissions even greater than that due to varying individual carbon cycle parameters (Fig. 1). Higher climate sensitivity means greater climate change, which enhances the positive feedback in the climate-carbon cycle system (Govindasamy et al., 2005), suppresses the long-term terrestrial sink and further reduces future permissible emissions. Permissible emissions are reduced still further, when values of climate sensitivity up to 10 K are considered. For climate sensitivities greater than 5.2 K (for 450 ppm) and 6.0 K (for 550 ppm) the cumulative emissions over the next three centuries are negative. This means that these high climate sensitivities imply a level of climate change sufficient to cause such rapid loss of terrestrial carbon that anthropogenic sequestration of CO_2 from the atmosphere would be required to maintain stabilized CO_2 levels. For all ecosystem parameter values and climate sensitivities considered here, the feedbacks imply much lower emissions than from studies which neglect climate change effects on the carbon cycle (Wigley et al., 1996).

4. Observational constraints

The simulations presented above exhibit significant differences in behaviour in terms of their spread of diagnosed anthropogenic emissions prior to present day. Hence, observations from the contemporary period may be used to eliminate some parameter combinations as being unrealistic, and therefore reduce uncertainty in future permissible emissions.

We extend our set of simulations with the simple model to vary multiple ecosystem parameters together, and use estimates of historical emissions to select combinations that recreate the historical record. Nine hundred model simulations were performed for each stabilization level, sampling all parameter value combinations of: q_{10} from (1.0, 1.5, 2.0, 2.5, 3.0 and 4.0), $C_{0.5}$ from (250, 375, 500, 625, 812.5 and 1000 ppm), d^2GPP/dT^2 from (−0.024, −0.018, −0.012, −0.006 and 0.0 K^{-2}) and T_{opt} from (−3.0, −1.5, 0.0, 1.5 and 3.0 K). Oceanic uptake of CO_2 is represented using an impulse-response approach after Joos et al. (1996). For the purpose of this study, uncertainty in this term is not considered. Although this is clearly an important source of uncertainty (e.g. Russell et al. in press, describe a possible negative feedback via Southern Ocean carbon uptake response to increased westerly winds), Friedlingstein et al. (2003, 2006) find that terrestrial uncertainty dominates the climate-carbon cycle feedback on the timescales of interest here.

We use estimates of historical anthropogenic emissions from 1860 to 2000 from fossil fuel and cement manufacture (Marland et al., 2005), and land-use change (Houghton and Hackler, 2002). Here,we choose to use just 70% of the estimated land-use emissions which may be overestimated due to northern forest regrowth (as explained in Jones et al., 2003a) but note that the main conclusions are not affected by this choice.

By selecting parameter combinations which match estimates of cumulative historical emissions to within 10 GtC we attempt to deduce possible combinations of parameter values and reduce uncertainty bounds on estimates of future permissible emissions. Uncertainty in historical emissions will reduce the ability of the record to constrain future permissible emissions, and is discussed later in this section.

Figure 2 shows the range of future permissible emissions when constrained by comparison with the historical emissions record. Despite the constrained agreement up to the present day, there is significant spread in future emissions. For a given value of climate sensitivity (the central dark-shaded region shows the projected range of permissible emissions when climate sensitivity is fixed at 3.0 K as calibrated against HadCM3LC), the use of the historical constraint has greatly reduced the spread of permissible emissions for each stabilization scenario compared with the unconstrained single-parameter variations shown in Fig. 1.

However, as has been discussed elsewhere (e.g. Andreae et al., 2005), the historical record is not able to tightly constrain climate sensitivity. Hence, a large spread of permissible emissions due to uncertain climate sensitivity remains. The paler shaded regions on Fig. 2 shows the projected permissible emissions for climate sensitivity within the IPCC-TAR range of 1.5–4.5 K. Even greater spread is obtained if climate sensitivities of up to 10 K are considered. For both stabilization scenarios, only climate sensitivities below 3.0 K allow any emissions above the WRE level, and even then only for a short period. By 2020 (WRE450) and 2050 (WRE550), respectively, all climate sensitivity values considered here imply emissions substantially below those of WRE. At higher climate sensitivities, emissions become negative for some period. This corresponds to a level of climate change that leads to sufficient loss of terrestrial carbon for it to be impossible to maintain stabilized atmospheric CO_2 concentrations without significant anthropogenic sequestration of CO_2 from the atmosphere. However, it should be noted that for such extreme cases of climate change which take the simple model well beyond its calibrated range, the results should be interpreted as illustrative rather than quantitatively robust. We note also that such high climate sensitivity, although not ruled out, is considered very unlikely. The important message from these results is that even moderate climate sensitivities imply significant

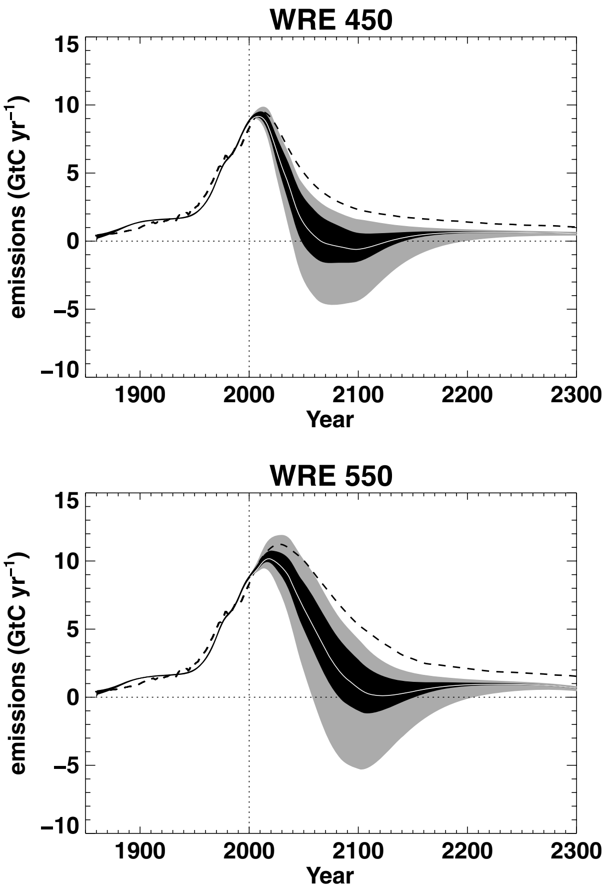

Fig. 2. Observationally constrained permissible emissions for WRE450 and WRE550 scenarios. Only parameter combinations which are consistent with historical emissions are chosen. The central white line represents the simple model results when run with the best fit parameters to HadCM3LC. The central black shading shows the uncertainty range for a climate sensitivity of 3 K (as fitted to HadCM3LC). The grey shading shows the range for climate sensitivity in the IPCC-TAR range of 1.5–4.5 K. The dashed lines show the emissions profiles from Wigley et al. (1996).

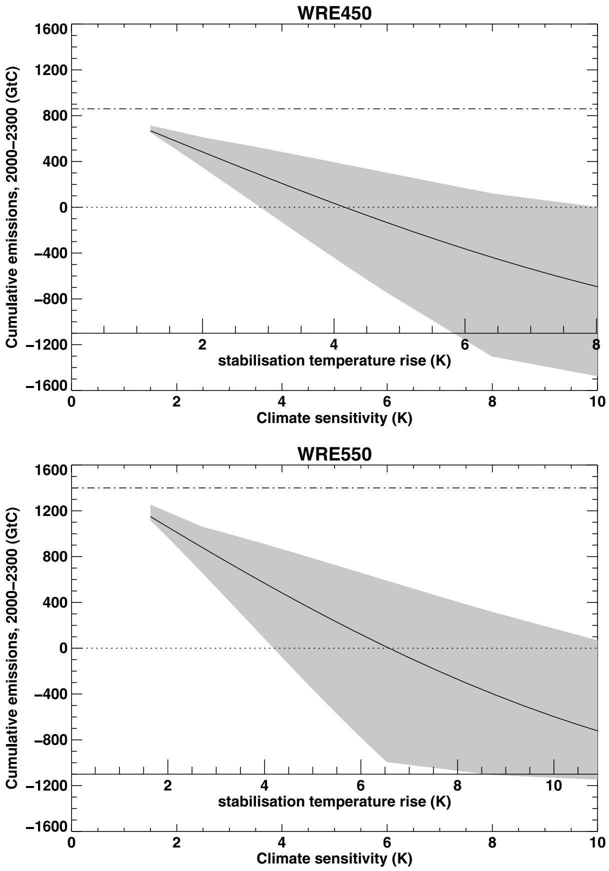

Fig. 3. Sensitivity of cumulative permissible CO_2 emissions from 2000 to 2300 to variations in the climate sensitivity. Results are shown for stabilization following WRE450 (top panel) and WRE550 (bottom panel) scenario. The solid lines show a strong decrease in cumulative emissions for increasing climate sensitivity when carbon cycle feedbacks are considered. Dot–dashed lines show values from Wigley et al. (1996) when these feedbacks are neglected. The shaded regions show the range of uncertainty when the carbon cycle parameters are varied, but constrained by the historical emissions. For reference, the global temperature change by 2300 is marked on a separate axis.

reductions in permissible emissions compared with the case of no feedbacks.

The very long-term limit to which permissible emissions approach is determined by the persistent natural sinks (Prentice et al., 2001) such as transport of anthropogenic carbon to the deep ocean. Since we are not perturbing ocean uptake behaviour in this study, our simulations begin to converge after about 2150.

The uncertainty bounds due to carbon cycle parameter uncertainty are themselves sensitive to the degree of climate change, and are much greater at higher climate sensitivities. This can be seen in Fig. 3 which shows uncertainty in the total cumulative emissions from 2000 to 2300 as a function of climate sensitivity. The solid lines correspond to simulations with the carbon cycle parameters fitted to HadCM3LC (as given above), and the dot–dashed lines show the corresponding WRE values. Shaded areas show the range of cumulative emissions when the carbon cycle parameters are varied, but constrained as above by comparison with historical emissions. For low climate sensitivity the carbon cycle parameters produce little spread because they are responding to much lower increases in global temperature. For high climate sensitivity (and hence much greater temperature rises), climate feedbacks have a stronger influence on the carbon cycle, and thus parameter uncertainty in the latter is reflected in larger uncertainty bounds on cumulative emissions. Figure 3 shows that for some carbon cycle parameters consistent with data from the contemporary period and at climate sensitivities towards the upper end of the range of the IPCC-TAR, stabilization at 450 ppm could only be achieved by engineered

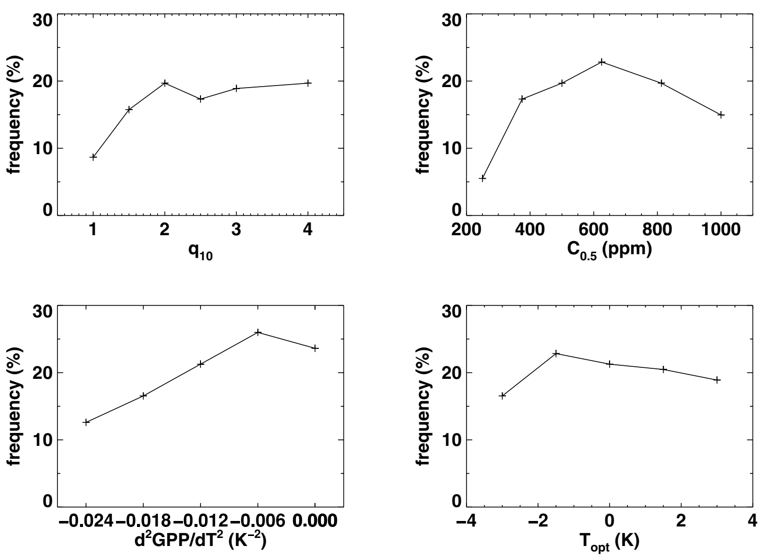

Fig. 4. Frequency distributions of each parameter. The figure shows the percentage frequency of occurrence of each parameter value within the set of 127 simulations which match the historical record of emissions. (a) q_{10}, (b) $C_{0.5}$, (c) d^2GPP/dT^2 and (d) T_{opt}.

sequestration of atmospheric CO_2 that is larger than total emissions between years 2000 and 2300 (i.e. the shaded region encompasses negative values for climate sensitivity values around 3.5–4.5 K).

Our hope when using the historical emissions record was to constrain parameters within the prior uncertainty range. It turns out that this is not possible. For each of the four carbon cycle parameters varied here, none of their ranges can be narrowed by the observational constraint.

The constraint does, however, allow two things. Firstly, it allows us to assess how often individual parameters are successful in recreating the historical emissions record. Figure 4 shows the frequency distribution of each parameter from all of the simulations which fit our criteria. One hundred and twenty-seven of the 900 parameter combinations match our chosen observational constraint. q_{10} exhibits roughly equal frequency of occurrence for values of q_{10} from 1.5 to 4. Only $q_{10} = 1$ is clearly less frequent than any of the other values. $C_{0.5}$ exhibits a broad peak in its frequency distribution with values of 500–800 ppm being more likely than 250 and 1000 ppm.

The curvature, d^2GPP/dT^2, of the sensitivity of productivity to climate shows more frequent occurrence at small magnitude than large, with a suggestion that the peak is distinct from zero. Values less than or equal to $-0.018\,K^{-2}$ occurring much less often. This suggests that the historical emissions record implies a likely upper limit on the magnitude of this parameter close to the value inferred from HadCM3LC ($-0.011\,K^{-2}$). This means that although the GCM sensitivity of productivity to climate is consistent with the observational record used here, it may be at the more sensitive end of the range. Matthews et al. (2005) investigated the impact of the productivity sensitivity to climate on the strength of climate-carbon cycle feedback in the UVic model, finding that the more sensitive the productivity, the greater the feedback strength. Our result here may help explain the strong HadCM3LC feedback within the C4MIP range of models (Friedlingstein et al., 2006).

The final panel in Fig. 4 shows the frequency distribution of the optimal temperature, T_{opt} from eq. (3). Here there is no clear information, with positive, negative and zero values occurring with similar frequency, although there is a suggestion of a peak around -1.5 K. Once again, the results of Matthews et al. (2005) show how important this parameter can be in determining the strength of climate-carbon cycle feedback. It appears that our comparison with the historical emissions record is not able to usefully constrain it.

Secondly, the observational constraint constrains combinations of parameters. For example, the observational record is consistent with both a high sensitivity of soil respiration to temperature and strong CO_2 fertilization or low sensitivity of both (i.e. either high q_{10} and $C_{0.5}$ or low q_{10} and $C_{0.5}$) but it is not consistent with high sensitivity of one and low sensitivity of the other. Figure 5 shows the frequency of occurrence of combinations of q_{10} and $C_{0.5}$ which allow the model to match the historical emissions record. Whilst both parameters can still vary within their full prior range, there are regions of parameter space which are not allowed or occur with much lower frequency—e.g. high q_{10} and low $C_{0.5}$ values or low q_{10} and high $C_{0.5}$ values are not consistent with the observational record. This joint constraint means that even though no individual parameter value can be ruled out, some combinations of values can be. Given that future feedback strength depends on the balance of these processes, the spread of future behaviour can thus be reduced. However, the non-linearity of eqs. (1) and (2) mean that combinations of q_{10} and $C_{0.5}$ which give similar past behaviour may give very different future behaviour. This may help explain the large spread of C4MIP results: many different models may give similar historical simulations but very different feedback strength in the future.

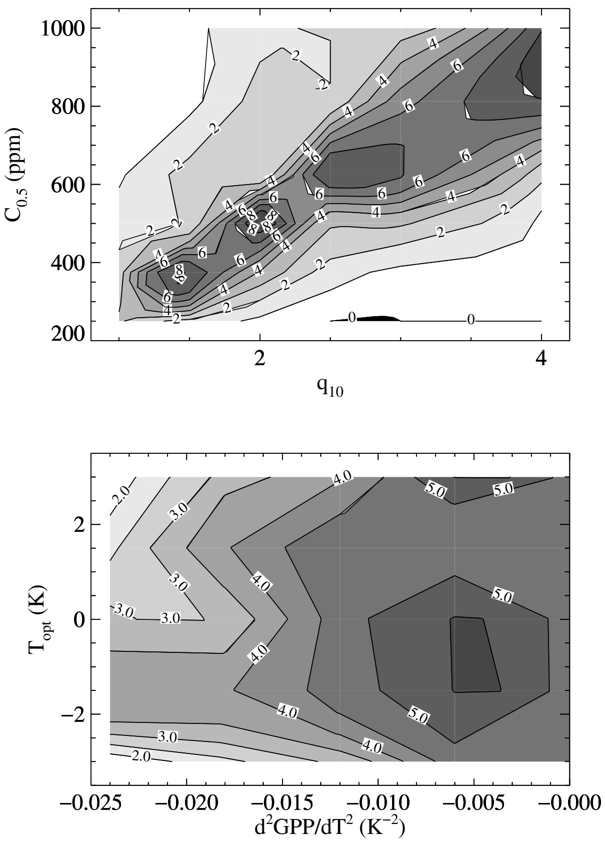

Fig. 5. Joint frequency distribution of (a) q_{10} and $C_{0.5}$ as constrained by the historical emissions record and (b) same for $\mathrm{d}^2\mathrm{GPP}/\mathrm{d}T^2$ and T_{opt}. The contours show the percentage frequency of occurrence of combinations of parameter values within the set of 127 simulations which match the historical record of emissions.

The joint constraint on $\mathrm{d}^2\mathrm{GPP}/\mathrm{d}T^2$ and T_{opt} (Fig. 5b) also shows more detail than is apparent from Fig. 4. The slight peak in T_{opt} at -1.5 K is more pronounced at greater absolute values of curvature. The more peaked the productivity dependence on climate, the more important the position of that peak.

The parameters fitted to HadCM3LC ($q_{10} = 2, C_{0.5} = 466$ ppm, $\mathrm{d}^2\mathrm{GPP}/\mathrm{d}T^2 = -0.011\,\mathrm{K}^{-2}$ and $T_{\mathrm{opt}} = 0\,\mathrm{K}$) fall close to the region of maximum frequency of occurrence showing that the GCM's behaviour is consistent with the observed record.

Our constraint here is to match anthropogenic carbon emissions over the historical period. The total emissions (about 380 GtC since 1860) is clearly uncertain, but by how much is not known, with land-use emissions in particular, poorly constrained. Our criteria of matching within 10 GtC will influence the inferred constraint. Matching much more closely would produce a more tightly, but spuriously, constrained future. Using less stringent criteria would allow a greater number of parameter combinations to fit the observations and reduce the future constraint. When the analysis was repeated using a criteria of ± 38 GtC (equivalent to 10% of the historical emissions) the results were qualitatively very similar. The optimal relationship between q_{10} and $C_{0.5}$ from Fig. 5 was unchanged, but the sharpness of the peak was reduced.

In this respect, there is an analogy with climate sensitivity: in the same way that imprecise knowledge of historical climate forcing restricts our ability to infer climate sensitivity, imprecise knowledge of historical carbon emissions restricts our ability to infer the carbon cycle sensitivity. Accurate observations of future emissions as well as future CO_2 levels are required to provide tighter constraints on global carbon cycle behaviour.

We also note that this study takes no account of uncertainty in ocean carbon uptake, which is likely to be substantial and will be investigated in future work. Hence it is likely that the carbon cycle behaviour cannot be well constrained using just global scale observations. The ability for global climate-carbon cycle models to recreate the historical climate and CO_2 record is a necessary, but far from sufficient condition on their reliability. Melnikov and O'Neill (2006) reach a similar conclusion that global carbon budgets offer only limited constraint on future carbon cycle behaviour. Even if the current budget was precisely known much future uncertainty remains. Better constraint of the carbon cycle can only come from improved process understanding and evaluation of models against a range of data such as land/ocean partitioning, interhemispheric and seasonal gradients, fine-scale flux tower measurements or the response to climate variability such as ENSO.

5. Intermodel uncertainty

The stated aim of the parameter perturbation experiments presented above was to try to span the uncertainty in permissible emissions due to uncertainty in process sensitivity to CO_2 and climate. However, the results are still dependent on a small number of fixed equations in a very simplified representation of the climate-carbon cycle system. The growing number of global climate-carbon cycle models allows us to assess uncertainty between models which differ structurally in both their representation of climate and the carbon cycle.

The C4MIP project (Friedlingstein et al., 2006) includes results from seven carbon cycle GCMs and four earth system models of intermediate complexity (EMICs). The results from transient experiments specifying CO_2 emissions according to the SRES-A2 scenario (Nakićenović et al., 2000) show a unanimous agreement that climate change exerts a positive feedback on the carbon cycle. But large disagreement remains on the magnitude of this feedback strength.

In the context of stabilization this translates into an agreement that climate feedbacks on the carbon cycle will lead to some reduction of permissible emissions, but by a very uncertain amount. Results similar to those from HadCM3LC have been obtained using the UVic model (Matthews, 2005) for stabilization at 1000 ppm. By taking the results of Matthews (2005) and scaling accordingly based on the feedback gain factor, g,

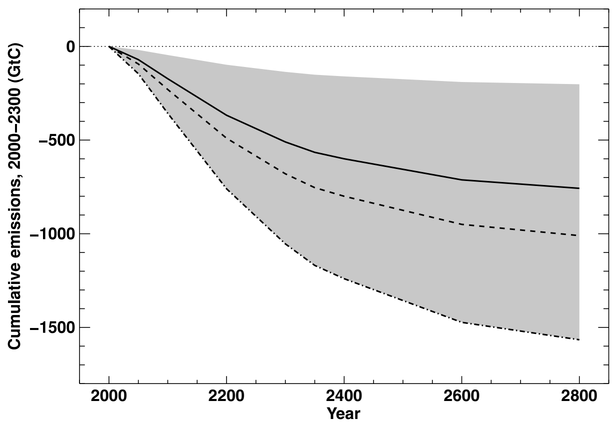

Fig. 6. Between–model uncertainty in reductions in permissible emissions. The reduction in cumulative emissions from 2000 to 2800 due to climate carbon cycle feedbacks for each of the C4MIP models was reconstructed for stabilization at 1000 ppm (see text). The shading represents the full C4MIP range. HadCM3LC (dot–dashed line) forms the bottom of this range as it has the strongest feedback and hence the greatest reductions. The dashed line shows the UVic results from Matthews (2005), and the solid line shows the C4MIP mean.

of Friedlingstein et al. (2006) we can reconstruct the permissible emissions that would be simulated by each C4MIP model under similar stabilization scenarios. Although somewhat simplistic, such a reconstruction worked well for results using our simple model, and so when applied to other models the results can be taken as a good approximation of the levels of emissions reductions.

Figure 6 shows the reconstructed C4MIP uncertainty range of cumulative emissions reductions due to climate-carbon cycle feedbacks by 2800, after stabilization of CO_2 at 1000 ppm by the year 2350. The results from Matthews (2005) for the UVic model ($g = 0.20$) indicate reductions of just over 1000 GtC. The equivalent emissions reduction from HadCM3LC is 1566 GtC ($g = 0.31$)—this is the largest level of reductions of the C4MIP model range. The minimum of the range has $g = 0.04$ and predicts emissions reductions of 202 GtC. Taking a simple mean and standard deviation of the C4MIP models ($g = 0.15 \pm 0.08$) implies a reduction of 758 ± 404 GtC.

In a similar study to ours, Eliseev and Mokhov (in press) use parameter perturbations in a simple coupled climate-carbon cycle model to explore future feedback strength. Their model is able to span the range of feedback strength seen in the C4MIP study. They find, similar to us, that constraints from observations of CO_2 are unable to well constrain future feedback strength. Such simple models are useful tools for us to be able to readily explore and analyse the sensitivity of carbon cycle feedbacks to model processes.

Future work to calibrate the simple model against each of the C4MIP members would help to provide a more precise comparison of their relative impacts on permissible stabilization emissions. Comparing the diagnosed q_{10}, $C_{0.5}$, d^2GPP/dT^2, and T_{opt} from each C4MIP model against the frequency distributions shown in Fig. 5 may help constrain the spread of C4MIP results.

6. Conclusions

Positive climate-carbon cycle feedbacks mean that permissible emissions must be substantially lower than previously expected. We have used a simple coupled climate-carbon cycle model calibrated against the HadCM3LC GCM to analyse the uncertainty bounds on such reductions due to uncertainty in physical and biogeochemical processes. All realistic carbon cycle feedbacks consistent with the observational record give permissible emissions much less than previously assumed, although uncertainties in carbon cycle parameters lead to relatively large uncertainty over future projections of permissible emissions.

Observational constraints provide some information on how parameters must co-vary by ruling out some combinations of parameter values (such as high q_{10} and low $C_{0.5}$). However, constraints from the observational record are not sufficient to narrow individual ranges of parameters beyond the arbitrary range chosen here.

Similar large uncertainty is found when comparing results between the different climate-carbon cycle models of the C4MIP project. An important next step is to identify process based observations which can constrain the behaviour of these models and reduce the uncertainty in future projections of the climate-carbon cycle feedback.

For a given level of climate sensitivity (and hence climate change at stabilization), the observational constraints are partially successful at reducing future uncertainty in permissible emissions. However, climate sensitivity cannot be well constrained by observations and so uncertainty in this quantity dominates uncertainty in future permissible emissions. Studies of past climates along with in-situ studies of cloud microphysics and large-scale studies of the effects of aerosols on cloud properties may help to reduce this uncertainty. As future GHG and aerosol forcing are expected to diverge (Andreae et al., 2005) and because future carbon cycle feedbacks are dependent on the degree of climate change, both the physical and biogeochemical components of the Earth System will become more strongly dependent on climate sensitivity. Thus, refining our estimate of this quantity is more crucial than ever.

7. Acknowledgments

This work was supported by the UK Department for Environment, Food and Rural Affairs Climate Prediction Program, under contract PECD 7/12/37. We are grateful to Damon Matthews for providing UVic model data used in Section 5. We gratefully acknowledge helpful comments from two anonymous reviewers.

8. Appendix. Simple model description

To complement the very computationally expensive fully coupled GCM experiments, a simple model was devised which could be used to emulate the GCM's behaviour and sensitivity to parameters (see also Jones et al., 2003b).

We consider the total carbon stored in vegetation, C_{v}, which is increased by photosynthesis, Π, and reduced by plant respiration, R_{p}, and litterfall, Λ:

$$\frac{\mathrm{d}C_{\mathrm{v}}}{\mathrm{d}t} = \Pi - R_{\mathrm{p}} - \Lambda, \tag{A1}$$

where Π is sometimes called GPP. In common with many others (McGuire et al., 1992; Collatz et al., 1991, 1992; Sellers et al., 1996; Cox et al., 1998), we assume that GPP depends directly on the atmospheric CO_2 concentration, C_a, and the climate:

$$\Pi = \Pi_{\max}\left(\frac{C_a}{C_a + C_{0.5}}\right) f(T), \tag{A2}$$

where $\Pi_{\max}$ is the value towards which GPP asymptotes as $C_a \to \infty$ and $C_{0.5}$ is the 'half-saturation' constant (i.e. the value of C_a for which Π is half this maximum value). The climate dependence of GPP is represented by f which can be considered as an arbitrary function of mean temperature, T, because regional climate change patterns (including those in precipitation) have been found to scale almost linearly with temperature (Huntingford et al., 2000). In this study, we choose this to be parabolic (see eq. 3).

Plant respiration is taken as the sum of a maintenance component, which depends on vegetation carbon and temperature, and a growth component, which is 25% of the remaining assimilate (once the maintenance respiration has been removed). This part of the model is identical to that used in the full TRIFFID dynamic global vegetation model (Cox, 2001). Annual litterfall is a fixed fraction of the vegetation carbon, $\Lambda = C_{\mathrm{v}}/\tau_{\mathrm{v}}$.

Soil carbon, C_{s}, evolves as a balance between organic litter input and heterotrophic respiration, R_{s} which is proportional to the soil carbon amount and a specific respiration rate given by a 'Q10' dependence (see eq. 2).

Surface air temperature is assumed to respond to changes in the atmospheric CO_2 concentration, C_a, as given by a simple heat capacity relationship (see box 1 of Andreae et al., 2005) which depends on the climate sensitivity to doubling atmospheric CO_2, $\Delta T_{2\times}$.

Fixed values of the terrestrial fluxes and stores were used to determine the turnover times, specific respiration rates for soil and vegetation carbon and $\Pi_{\max}$. When perturbations are applied to $C_{0.5}$, $\Pi_{\max}$ is automatically perturbed too, in order to maintain constant initial conditions of productivity and vegetation carbon storage across all simulations.

The impulse-response ocean uptake model was as given by Joos et al. (1996) for a 3D ocean model, but with a reduced 'mixed layer depth' of 40 metres to capture lower ocean uptake rates in HadCM3LC. The ocean was also assumed to experience a lower degree of warming than the land (by a factor of 1.87) in line with the full GCM results (Huntingford et al., 2000). This warming influences the uptake of carbon through the impact of the mean ocean temperature on the solubility of CO_2 in seawater (Joos et al., 1996).

This simple model was calibrated against full HadCM3LC results with and without climate feedbacks on the carbon cycle (Cox et al., 2000), and then tested to see how well it reproduced the different behaviour associated with stabilization scenarios. The results show it has been successful in being able to emulate the GCM behaviour (Jones et al., 2006).

References

Andreae, M. O., Jones, C. D. and Cox, P. M. 2005. Strong present-day aerosol cooling implies a hot future. *Nature* **435**, 1187–1190.

Andronova, N. G. and Schlesinger, M. E. 2001. Objective estimation of the probability density function for climate sensitivity. *J. Geophys. Res.* **106**, 22 605–22 612.

Annan, J. and Hargreaves, J. C. 2006. Using multiple observationally-based constraints to estimate climate sensitivity. *Geophys. Res. Lett.* **33**, L06704. doi:10.1029/2005GL025259.

Annan, J. D., Hargreaves, J. C., Ohgaito, R., Abe-Ouchi, A. and Emori, S. 2005. Efficiently constraining climate sensitivity with ensembles of paleoclimate simulations. *SOLA* **1**, 181–184.

Collatz, G. J., Ball, J. T., Grivet, C. and Berry, J. A. 1991. Physiological and environmental regulation of stomatal conductance, photosynthesis and transpiration: A model that includes a laminar boundary layer. *Agric. For. Meteorol.* **54**, 107–136.

Collatz, G. J., Ribas-Carbo, M. and Berry, J. A. 1992. A coupled photosynthesis-stomatal conductance model for leaves of C_4 plants. *Aust. J. Plant Physiol.* **19**, 519–538.

Cox, P. M. 2001. *Description of the TRIFFID Dynamic Global Vegetation Model*, Technical Note 24, Hadley Centre, Met Office.

Cox, P. M., Betts, R. A., Jones, C. D., Spall, S. A. and Totterdell, I. J. 2000. Acceleration of global warming due to carbon–cycle feedbacks in a coupled climate model. *Nature* **408**, 184–187.

Cox, P. M., Betts, R. A., Jones, C. D., Spall, S. A. and Totterdell, I. J. 2001. Modelling vegetation and the carbon cycle as interactive elements of the climate system. In: *Meteorology at the Millennium* (ed. R. Pearce), pp. 259–279. Academic Press, London.

Cox, P. M., Huntingford, C. and Harding, R. J. 1998. A canopy conductance and photosynthesis model for use in a GCM land surface scheme. *J. Hydrol.* **212–213,** 79–94.

Eliseev, A. V. and Mokhov, I. I. 2006. Carbon cycle-climate feedback sensitivity to parameter changes of a zero-dimensional terrestrial carbon cycle scheme in a climate model of intermediate complexity. *Theor. Appl. Climatol.,* in press.

Forest, C. E., Stone, P. H., Sokolov, A. P., Allen, M. R. and Webster, M. D. 2002. Quantifying uncertainties in climate system properties with the use of recent climate observations. *Science* **295**, 113–117.

Friedlingstein, P., Bopp, L., Ciais, P., Dufresne, J.-L., Fairhead, L. and co-authors. 2001. Positive feedback between future climate change and the carbon cycle. *Geophys. Res. Lett.* **28**, 1543–1546.

Friedlingstein, P., Cox, P. M., Betts, R. A., Bopp, L., von Bloh, W. and co-authors. 2006. Climate–carbon cycle feedback analysis, results from the C4MIP model intercomparison. *Journal of Climate,* **Vol. 19**, No. 14, pp. 3337–3353. doi:10.1175/JOL13800.1.

Friedlingstein, P., Dufresne, J. L., Cox, P. M. and Rayner, P. 2003. How positive is the feedback between climate change and the carbon cycle?. *Tellus* **55B,** 692–700.

Gordon, C., Cooper, C., Senior, C. A., Banks, H., Gregory, J. M. and co-authors. 2000. The simulation of SST, sea ice extents and ocean heat transports in a version of the Hadley Centre coupled model without flux adjustments. *Climate Dyn.* **16**, 147–168.

Govindasamy, B., Thompson, S., Mirin, A., Wickett, M., Caldeira, K. and co-authors. 2005. Increase of carbon cycle feedback with climate sensitivity: results from a coupled climate and carbon cycle model. *Tellus* **57B,** 153–163.

Gregory, J. M., Stouffer, R. J., Raper, S. C. B., Stott, P. A. and Rayner, N. A. 2002. An observationally based estimate of the climate sensitivity. *J. Climate* **15**, 3117–3121.

Harvey, L. D. D. and Kaufmann, R. K. 2002. Simultaneously constraining climate sensitivity and aerosol radiative forcing. *J. Climate* **15**, 2837–2861.

Hegerl, G. C., Crowley, T. J., Hyde, W. T. and Frame, D. J. 2006. Climate sensitivity constrained by temperature reconstructions over the past seven centuries. *Nature* **440**, 1029–1032.

Houghton, J. T., Ding, Y., Griggs, D. J., Noguer, M., van der Linden, P. and co-authors. 2001. *Climate Change 2001: the scientific basis. Contribution of Working Group 1 to the Third Assessment Report of the Intergovernmental Panel on Climate Change*. Cambridge University Press, Cambridge, UK.

Houghton, R. A. and Hackler, J. L. 2002. Carbon flux to the atmosphere from land-use changes. In: *Trends: A Compendium of Data on Global Change*, Carbon Dioxide Information Analysis Center.

Huntingford, C. and Cox, P. M. 2000. An analogue model to derive additional climate change scenarios from existing GCM simulations. *Clim. Dyn.* **16**, 575–586.

Huntingford, C., Cox, P. M. and Lenton, T. M. 2000. Contrasting responses of a simple terrestrial ecosystem model to global change. *Ecol. Model.* **134**, 41–58.

Jones, C. D. and Cox, P. M. 2001. Constraints on the temperature sensitivity of global soil respiration from the observed interannual variability in atmospheric CO_2. *Atmos. Sci. Lett.* doi:10.1006/asle.2000.0041.

Jones, C. D., Cox, P. M., Essery, R. L. H., Roberts, D. L. and Woodage, M. J. 2003a. Strong carbon cycle feedbacks in a climate model with interactive CO_2 and sulphate aerosols. *Geophys. Res. Lett.* **30**, 10.1029/2003GL016867.

Jones, C. D., Cox, P. M. and Huntingford, C. 2003b. Uncertainty in climate-carbon cycle projections associated with the sensitivity of soil respiration to temperature. *Tellus* **55B,** 642–648.

Jones, C. D., Cox, P. M. and Huntingford, C. 2006. Impact of climate-carbon cycle feedbacks on emission scenarios to achieve stabilization. In: *Avoiding Dangerous Climate Change* Chapter 34 (eds. H. J. Schellnhuber, W. Cramer, N. Nakicenovic, T. Wigley and G. Yohe). Cambridge University Press, Cambridge.

Joos, F., Bruno, M., Fink, R., Siegenthaler, U., Stocker, T. F. and co-authors. 1996. An efficient and accurate representation of complex oceanic and biospheric models of anthropogenic carbon uptake. *Tellus* **48B,** 397–417.

Joos, F., Meyer, R., Bruno, M. and Leuenberger, M. 1999. The variability in the carbon sink as reconstructed for the last 1000 years. *Geophys. Res. Lett.* **26**, 1437–1440.

Knorr, W., Prentice, I. C., House, J. I. and Holland, E. A. 2005. Long-term sensitivity of soil carbon turnover to warming. *Nature* **433**, 298–301.

Knutti, R., Joos, F., Muller, S. A., Plattner, G. K. and Stocker, T. F. 2005. Probabilistic climate change projections for CO_2 stabilization profiles. *Geophys. Res. Lett.* **32**, 10.1029/2005GL023294.

Knutti, R., Stocker, T. F., Joos, F. and Plattner, G. K. 2002. Constraints on radiative forcing and future climate change from observations and climate model ensembles. *Nature* **416**, 719–723.

Marland, G., Boden, T. A. and Andres, R. J. 2005. Global, regional, and national fossil fuel CO_2 emissions In: *Trends: A Compendium of Data on Global Change*, Carbon Dioxide Information Analysis Center.

Mastrandrea, M. D. and Schneider, S. H. 2006. Probabilistic assessment of 'dangerous' climate change and emissions scenarios: Stakeholder metrics and overshoot pathways. In: *Avoiding Dangerous Climate Change* chapter 27 (eds.H. J. Schellnhuber, W. Cramer, N. Nakicenovic, T. Wigley and G. Yohe). Cambridge University Press, Cambridge.

Matthews, H. D. 2005. Decrease of emissions required to stabilize atmospheric CO_2 due to positive carbon cycle–climate feedbacks. *Geophys. Res. Lett.* **32**, 10.1029/2005GL023435.

Matthews, H. D. 2006. Emissions targets for CO_2 stabilization as modified by carbon cycle feedbacks. *Tellus* **58B,** this issue.

Matthews, H. D., Eby, M., Weaver, A. J. and Hawkins, B. J. 2005. Primary productivity control of the simulated climate-carbon cycle feedback. *Geophys. Res. Lett.* **32**, doi:10.1029/2005GL022941.

McCarthy, J. J., Canziani, O. F., Leary, N. A., Dokken, D. J. and White, K. S. 2001. *Climate Change 2001: Impacts, Adaptation and Vulnerability*, Cambridge University Press, Cambridge.

McGuire, A. D., Melillo, J. M., Joyce, L. M., Kicklighter, D. M., Grace, A. L., Moore, B. and Vorosmarty, C. J. 1992. Interactions between carbon and nitrogen dynamics in estimating net primary productivity for potential vegetation in North America. *Global Biogeochem. Cycles* **6**, 101–124.

Meinshausen, M. 2006. What does a 2 °C target mean for greenhouse gas concentrations? a briefanalysis based on multi-gas emission pathways and several climate sensitivity uncertainty estimates. In: *Avoiding Dangerous Climate Change* Chapter 28 (eds. H. J. Schellnhuber, W. Cramer, N. Nakicenovic, T. Wigley and G. Yohe). Cambridge University Press, Cambridge.

Melnikov, N. B. and O'Neill, B. C. 2006. Learning about the carbon cycle from global budget data. *Geophys. Res. Lett.* **33**, doi:10.1029/2005GL023935.

Murphy, J. M., Sexton, D. M. H., Barnett, D. N., Jones, G. S., Webb, M. J., Collins, M. and Stainforth, D. A. 2004. Quantification of modelling uncertainties in a large ensemble of climate change simulations. *Nature* **430**, 768–772.

Nakićenović, N., Alcamo, J., Davis, G., de Vries, B., Fenhann, J. and co-authors. 2000. *Special Report on Emissions Scenarios*, Cambridge University Press, Cambridge, 599pp.

Pachauri, R. 2006. Avoiding dangerous climate change. In: *Avoiding Dangerous Climate Change* Chapter 1 (eds. H. J. Schellnhuber, W. Cramer, N. Nakicenovic, T. Wigley and G. Yohe). Cambridge University Press, Cambridge.

Parker, D. E., Folland, C. K. and Jackson, M. 1995. Marine surface temperature: observed variations and data requirements. *Clim. Change* **31**, 559–600.

Prentice, I. C., Farquhar, G. D., Fasham, M. J. R., Goulden, M. L., Heimann, M. and co-authors. 2001. The carbon cycle and atmospheric carbon dioxide. In: *Climate Change 2001: The scientific basis. Contribution of Working Group I to the Third Assessment Report of the Intergovernmental Panel on Climate Change* Chapter 3 (eds. J. T. Houghton, Y. Ding, D. J. Griggs, M. Noguer, P. van der Linden, X. Dai, K. Maskell, and C. I. Johnson). pp. 183–237, Cambridge University Press.

Russell, J. L., Dixon, K. W., Gnanadesikan, A., Stouffer, R. J. and Toggweiler, J. R. 2006. The southern hemisphere westerlies in a warming world: Propping open the door to the deep ocean. *J. Climate*, in press.

Schneider, S. H. and Lane, J. 2006. An overview of dangerous climate change. In: *Avoiding Dangerous Climate Change* Chapter 2 (eds. H. J. Schellnhuber, W. Cramer, N. Nakicenovic, T. Wigley and G. Yohe). Cambridge University Press, Cambridge.

Sellers, P. J., Randall, D. A., Collatz, C. J., Berry, J. A., Field, C. B. and co-authors. 1996. A revised land surface parameterization (SiB2) for atmospheric GCMs. Part I: Model formulation. *J. Climate* **9**, 676–705.

Stainforth, D. A., Aina, T., Christensen, C., Collins, M., Frame and co-authors. 2005. Uncertainty in predictions of the climate response to rising levels of greenhouse gases. *Nature* **433**, 403–406.

Thompson, S. L., Govindasamy, B., Mirin, A., Caldeira, K., Delire, C. and co-authors. 2004. Quantifying the effects of CO_2-fertilized vegetation on future global climate and carbon dynamics. *Geophys. Res. Lett.* **31**, doi:10.1029/2004GL021239.

von Deimling, T. S., Held, H., Ganopolski, A. and Rahmstorf, S. 2006. Climate sensitivity estimated from ensemble simulations of glacial climate. *Clim. Dyn.* **27.** 149–163. doi:10.1007/s00382-006-0126–8.

Wigley, T. M. L., Richels, R. and Edmonds, J. A. 1996. Economic and environmental choices in the stabilization of atmospheric CO_2 concentrations. *Nature* **379**, 242–245.

Zeng, N., Qian, H., Munoz, E. and Iacono, R. 2004. How strong is carbon cycle-climate feedback under global warming? *Geophys. Res. Lett.* **31**, doi:10.1029/2004GL020904.